Bio-Design and Manufacturing (2024) 7:637–650
https://doi.org/10.1007/s42242-024-00288-0

RESEARCH ARTICLE

Kinematics of mandibular advancement devices (MADs): Why do some MADs move the lower jaw backward during mouth opening?

Juan A. Cabrera[1] · Alex Bataller[1] · Sergio Postigo[1] · Marcos García[1]

Received: 17 October 2023 / Accepted: 8 May 2024 / Published online: 27 August 2024

Abstract

Mandibular advancement devices (MADs) are widely used treatments for obstructive sleep apnea. MADs function by advancing the lower jaw to open the upper airway. To increase patient comfort, most patients allow the mouth to be opened. However, not all systems maintain the lower jaw in a forward position during mouth opening, which results in the production of a retrusion that favors the collapse of the upper airway. Furthermore, the kinematic behavior of the mechanism formed by the mandible-device assembly depends on jaw morphology. This means that, during mouth opening, some devices cause lower jaw protrusion in some patients, but cause its retraction in others. In this study, we report the behavior of well-known devices currently on the market. To do so, we developed a kinematic model of the lower jaw device assembly. This model was validated for all devices analyzed using a high-resolution camera system. Our results show that some of the devices analyzed here did not produce the correct behavior during patient mouth opening.

Graphic abstract

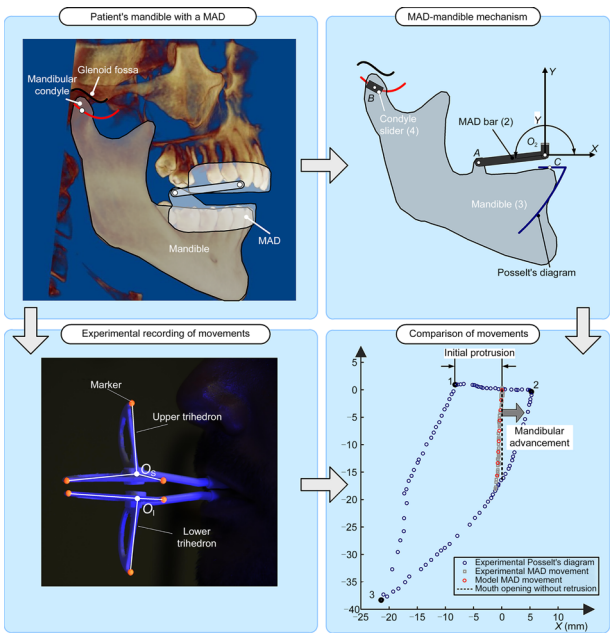

Keywords Mandibular advancement devices · Lower jaw kinematics · Sleep apnea

✉ Juan A. Cabrera
jcabrera@uma.es

[1] Mechanical Engineering Department, University of Malaga, 29071 Malaga, Spain

Introduction

Sleep apnea is a disorder in which breathing is interrupted while a person sleeps [1, 2]. The most common type of sleep apnea is obstructive sleep apnea (OSA), which involves a partial or complete collapse of the airway during sleep. Patients suffering from sleep apnea can suffer from excessive daytime sleepiness and are at a high risk of developing cardiovascular diseases including arrhythmias, heart failure, and stroke [3–5].

To solve this problem, specialists recommend using three different treatments: the use of continuous positive air pressure (CPAP) machines, the use of mandibular advancement devices (MADs), and surgery. CPAP machines are devices that produce a constant positive air pressure in the upper airway via a nose or face mask, thereby preventing its collapse. MADs cause the forward displacement of the lower jaw, which induces stretching of muscles that support the upper airway, thereby preventing its collapse. For the proper function of MADs, the lower jaw must remain in a forward position with the mouth closed and open. Compared to CPAP devices, MADs are easier to transport, do not produce noise, do not require electrical power to operate, and overall have a higher adherence rate [6]. One recent comprehensive study [7] compared different types of MADs, including both monoblock devices that restrict the mouth opening and two-piece devices which are categorized by their connection position (i.e., lateral or frontal). The findings of this study indicated that monoblock devices were more effective in reducing the average number of apneas and hypopneas during sleep, as measured by the apnea hypopnea index (AHI), than connected two-piece devices were. However, frontally connected devices showed the greatest reduction in AHI. However, instead of considering only the connection position, the linking mechanism should be considered to analyze the movements it induces during the opening of the mouth. This is since mandibular retrusion occurs in some cases, whereas in others, mandibular protrusion increases. Obviously, if the mouth cannot be opened, the initial protrusion is guaranteed to be maintained.

There are a large number of MADs currently on the market. Most are composed of two dental splints joined by different elements, such as rigid bars, telescopic bars, elastic straps, and flaps or cams [8]. The use of MADs is known to reduce the degree of freedom of the lower jaw and limit both mouth opening and lateral motion. However, many users prefer models that permit a wider range of mouth opening and/or lateral movement of the lower jaw. The two dental splints mentioned above are mounted on the upper (maxilla) and lower (mandible) dental arches. Their relative movement depends on three aspects: the mechanism by which they are joined to the two splints, the temporomandibular joint, and the patient's morphology. Therefore, each of these three aspects is necessary to determine whether a MAD will function correctly in a given patient when opening the mouth [9]. Moreover, this may explain why the effectiveness of MADs can vary depending on the patient [10, 11].

Furthermore, to the best of our knowledge, only one MAD currently available on the market is manufactured after considering the morphology of each patient and the kinematics of his/her lower jaw movement [12], and involves the use of a cam-follower mechanism. Lower jaw kinematics has been used in other fields, including robotics and the modeling of mastication processes [13–18], in order to design mechanisms and robots that adjust to movements performed by the lower jaw. Determining these movements and their limits is fundamental for the development of any device, mechanism, or robot that attempts to control or reproduce the movement of the lower jaw.

One of the first researchers to study mandible kinematics was Posselt, who studied the border movements of the lower incisor in the sagittal, frontal, and lateral planes [19]. Posselt concluded that the lower jaw movement in the sagittal plane is a characteristic that is specific to each individual. This movement defines an area with three borders that are described by the trajectory of the tip of the lower incisor when moving the mandible from the most retruded to the most protruded positions with the mouth closed (upper border), maintaining maximum protrusion when opening the mouth to its maximum (anterior border), and closing the mouth while keeping the mandible in the most retruded position possible (posterior border). Many research groups have attempted to reproduce these diagrams using devices mounted on dental arches, and these studies have contributed to achieving a better knowledge of lower jaw movement [20–23].

In this work, we conduct a complete study of the most representative mandibular advancement devices currently on the market and analyze their behavior in a specific patient. To do so, we track the movement of the mechanical assembly formed by the mandible and each device in the sagittal plane, and analyze the degrees of freedom of the resulting mechanism and its kinematic joints. By obtaining estimate of mandibular movement during use of a MAD, it is possible to predict whether the device will behave correctly in the patient under study.

The contributions of this work are as follows:

- Develop a kinematic model of the mandible when a patient uses a certain mandibular advancement device. This study will be conducted in the sagittal plane because this motion determines the correct or incorrect functioning of the device.
- Validate the kinematic model using camera measurements of lower jaw movement for each of the different MADs analyzed.

- Determine the lower incisor trajectory for each device. We answer the question: why do some devices move the lower jaw backward during patient mouth opening?
- Discuss solutions to device malfunctioning.

Accordingly, this work is organized as follows. In the "Methods" section, we describe the methodology used to characterize the complete jaw movement for the most common mandibular advancement devices. We then present generalized coordinates and equations that solve the kinematics of each model. In the "Results" section, the kinematic models are validated using a camera measurement system and a trihedron with markers. The results obtained from the real tests are then compared with those obtained by the proposed kinematic models. Discussion of these results is provided in the "Discussion" section. Finally, conclusions are drawn in the "Conclusions" section.

Methods

To model the kinematic behavior of the mandible when using a mandibular advancement device, we used the following procedure (Fig. 1a):

- A lateral X-ray or scan of the patient was taken parallel to the sagittal plane.
- A mathematically defined shape of the glenoid fossa was fitted to a series of points marked on an X-ray or scan.
- The trajectory of the geometric center of the condyle was identified from the lateral X-ray. For this purpose, we assumed that the distance from the glenoid curve obtained in the previous step is constant.
- The mandibular advancement device was placed on the patient's mandible and maxilla.

Once these steps were performed, we obtained an equivalent mechanism that replicates lower jaw movement in the sagittal plane when the patient uses a given MAD (Fig. 1b). Analysis of this mechanism allows us to obtain the specific curve created by the tip of the patient's lower incisor when opening the mouth. This will thus verify whether the mandible protrudes or recedes.

Device deformation was not considered since the MADs studied in this work use class II-a biocompatible materials, which have a high degree of stiffness [24].

Mechanism for a MAD with bars

The mechanical system of a MAD with bars (Fig. 1) consists of the following kinematic pair and the resulting system has one degree of freedom:

- A rotational kinematic pair formed by the maxilla, a MAD bar, and a hinge at point O_2.
- A rotational kinematic pair including the bar, mandible, and a hinge at point A.
- A prismatic kinematic pair formed by a slider and the glenoid fossa, which simulates the movement of the condyle center along a path parallel to the glenoid fossa.
- A rotational kinematic pair consisting of the mandible, the slider used to achieve the movement of the condyle, and a hinge at point B.

This equivalent mechanism has one degree of freedom and can be modeled using the following generalized coordinates [25]:

$$q = \{x_A,\ y_A,\ x_B,\ y_B,\ x_C,\ y_C,\ \gamma\}. \tag{1}$$

Here, (x_A, y_A), (x_B, y_B), and (x_C, y_C) are coordinates in the sagittal plane of points A, B, and C, respectively, and γ is the angle between the bar and the X axis.

Since there are seven coordinates and the mechanism has one degree of freedom, six constraint equations are needed:

$$\left(x_{O_2} - x_A\right)^2 + \left(y_{O_2} - y_A\right)^2 - L_{O_2A}^2 = 0, \tag{2}$$

$$(x_A - x_B)^2 + (y_A - y_B)^2 - L_{AB}^2 = 0, \tag{3}$$

$$(x_B - x_C)^2 + (y_B - y_C)^2 - L_{BC}^2 = 0, \tag{4}$$

$$(x_C - x_A)^2 + (y_C - y_A)^2 - L_{CA}^2 = 0, \tag{5}$$

$$y_B - \left(ax_B^3 + bx_B^2 + cx_B + d\right) = 0, \tag{6}$$

$$\left(x_A - x_{O_2}\right) - L_{O_2A}\cos\gamma = 0. \tag{7}$$

Equation (2) defines the rigid solid condition of the bar, given that its length L_{O_2A} and the position of point O_2 are known. Equations (3)–(5) define the rigid solid condition of the mandible, and here lengths L_{AB}, L_{BC}, and L_{CA} are known since they can be measured by X-ray. Equation (6) indicates that point B must lie on the curve of the trajectory of the center of the condyle which is fitted by a third-degree polynomial with parameters a, b, c, and d known. Finally, Eq. (7) defines the angle between the bar and the X axis. Once all constraints are defined, a Newton–Raphson iterative process is used to solve the position of the mechanism using the following equation:

$$\Phi_q(q) \cdot (q_{i+1} - q_i) = -\Phi(q). \tag{8}$$

Here, q is the set of natural coordinates defined in Eq. (1), $\Phi(q)$ is the set of constraints defined in Eqs. (2)–(7), and

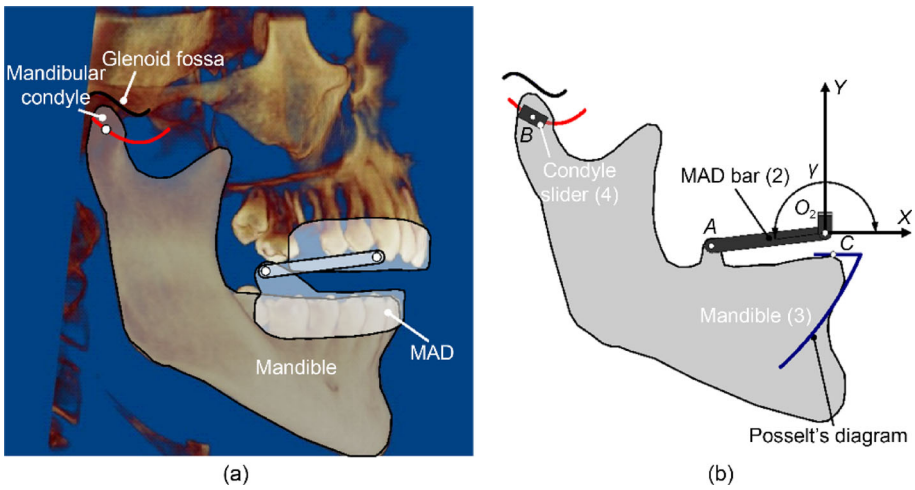

Fig. 1 Methodology for mechanistic modeling of the assembly formed by the lower jaw and a MAD: **a** patient scan with a sketch of the mounted MAD; **b** equivalent mechanism reproducing the movement of the lower jaw with a MAD with bars. MAD: mandibular advancement device

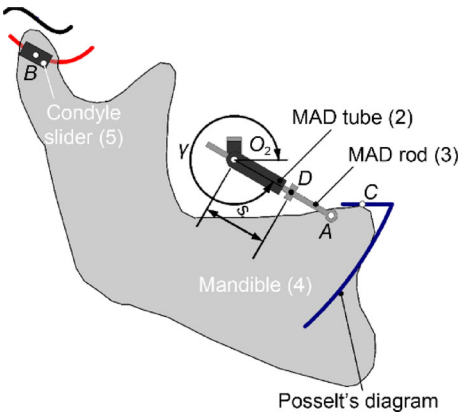

Fig. 2 Equivalent mechanism that replicates the kinematic behavior of the lower jaw using a telescopic bar device. MAD: mandibular advancement device

$\Phi_q(q)$ is the Jacobian of the set of constraints with respect to the coordinates. To solve Eq. (8), we introduce an initial value set for the coordinates, $q_i = \{x_A^i, y_A^i, x_B^i, y_B^i, x_C^i, y_C^i\}$, with angle γ as the input value of the degree of freedom of the mechanism. We then obtain, using an iterative process, the final value of the coordinates, $q_{i+1} = \{x_A^{i+1}, y_A^{i+1}, x_B^{i+1}, y_B^{i+1}, x_C^{i+1}, y_C^{i+1}\}$. This procedure can then be carried out with all input angles γ, determining the movement of any point on the lower jaw. Next, we analyze the movement of point C (tip of the lower incisor) since its trajectory is used to determine whether mandible retrusion or protrusion occurs when a patient opens his/her mouth.

Mechanisms with telescopic bars

The mechanical system formed by the telescopic bar device and the lower jaw in the sagittal plane has two degrees of freedom (Fig. 2). In this case, the generalized coordinates required to model the mechanism are:

$$q = \{x_A, y_A, x_B, y_B, x_C, y_C, x_D, y_D, s, \gamma\}. \tag{9}$$

Since there are 10 coordinates and two degrees of freedom, eight constraint equations are required to define constraint set $\Phi(q)$:

$$(x_A - x_C)^2 + (y_A - y_C)^2 - L_{AC}^2 = 0, \tag{10}$$

$$(x_A - x_B)^2 + (y_A - y_B)^2 - L_{AB}^2 = 0, \tag{11}$$

$$(x_B - x_C)^2 + (y_B - y_C)^2 - L_{BC}^2 = 0, \tag{12}$$

$$(x_A - x_D)^2 + (y_A - y_D)^2 - L_{AD}^2 = 0, \tag{13}$$

$$(x_D - x_{O_2})(y_A - y_{O_2}) - (y_D - y_{O_2})(x_A - x_{O_2}) = 0, \tag{14}$$

$$y_B - \left(ax_B^3 + bx_B^2 + cx_B + d\right) = 0, \tag{15}$$

$$(x_A - x_{O_2}) - (s + L_{AD})\cos\gamma = 0, \tag{16}$$

$$(x_D - x_{O_2}) - \frac{s}{L_{O_2A}}(x_A - x_{O_2}) = 0. \tag{17}$$

As in the previous case, Eqs. (10)–(12) define the rigid solid condition of the lower jaw. Equation (13) defines the rigid solid condition of link 3 (rod) of the MAD mechanism, where L_{AD} is known. Equation (14) establishes the sliding condition between link 3 (rod) and link 2 (tube). Equation (15) establishes the condition that point B must be in the center of the path of the condyle, which is defined by the known parameters a, b, c, and d. Equation (16) establishes angle γ between link 2 and the X axis. Finally, Eq. (17) establishes linear displacement s between links 2 and 3.

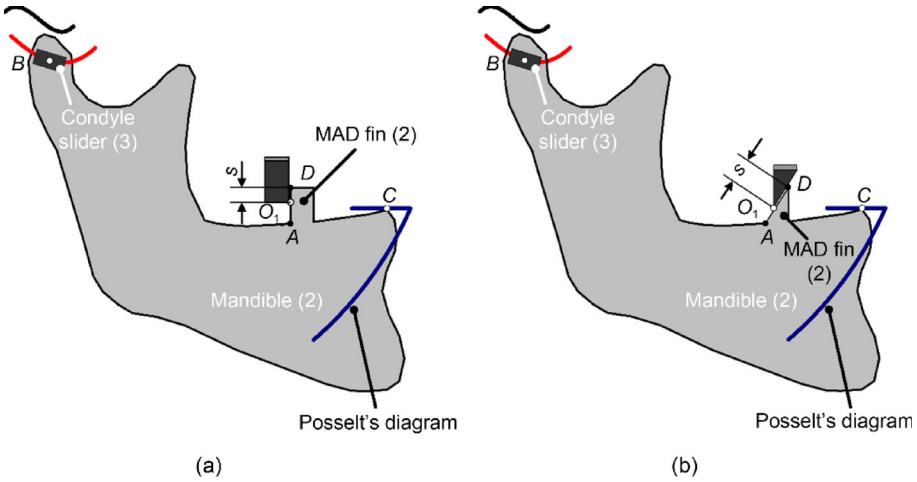

Fig. 3 Equivalent mechanism for devices with straight fins: **a** vertical profile (ProSomnus EVO); **b** angled profile (SomnoDent Flex). MAD: mandibular advancement device

As in the previous case, the movement of the mechanism was obtained by using an iterative process and solving Eq. (8). However, in this case, the system has two degrees of freedom, so two new input variables (i.e., γ and s) are included in the system.

Mechanisms with straight fins

Two mechanisms that include fins (shown in Fig. 3) are the most common on the market and have one degree of freedom. In both cases, cams with a straight profile defined by points A and D are used, with O_1 being the point of contact between the fin that is attached to the lower jaw and the fin that is attached to the maxilla.

The generalized coordinates used for devices with straight fins are:

$$q = \{x_A,\ y_A,\ x_B,\ y_B,\ x_C,\ y_C,\ x_D,\ y_D,\ s\}. \tag{18}$$

As in the previous cases, we first define the set of constraints $\Phi(q)$, represented using the following equations:

$$(x_A - x_B)^2 + (y_A - y_B)^2 - L_{AB}^2 = 0, \tag{19}$$

$$(x_A - x_C)^2 + (y_A - y_C)^2 - L_{AC}^2 = 0, \tag{20}$$

$$(x_B - x_C)^2 + (y_B - y_C)^2 - L_{BC}^2 = 0, \tag{21}$$

$$(x_D - x_A) - \lambda(x_B - x_A) - \mu(x_C - x_A) = 0, \tag{22}$$

$$(y_D - y_A) - \lambda(y_B - y_A) - \mu(y_C - y_A) = 0, \tag{23}$$

$$(x_D - x_A)\left(y_{O_1} - y_A\right) - (y_D - y_A)\left(x_{O_1} - x_A\right) = 0, \tag{24}$$

$$y_B - \left(ax_B^3 + bx_B^2 + cx_B + d\right) = 0, \tag{25}$$

$$\left(x_D - x_{O_1}\right) - \frac{s}{L_{AD}}(x_D - x_A) = 0. \tag{26}$$

Here, Eqs. (19)–(21) define the rigid solid condition of the lower jaw when the lengths L_{AB}, L_{AC}, and L_{BC} are known. Equations (22) and (23) define the position of point D in a plane defined by points A, B, and C, and λ and μ are parameters with known values. Equation (24) specifies that point O_1 always lies on straight line AD. Equation (25) establishes the condition that point B must always lie on the trajectory of the condyle, defined by the known parameters a, b, c, and d. Finally, Eq. (26) establishes the contact length of the cam.

Mechanisms with curved fins

We analyzed a curved fin device called Orthoapnea NOA that uses a curved cam profile designed with a protrusive trajectory for the tip of the patient's lower incisor when the mouth is opened [12]. By considering the specific morphology of each patient, the cam profile is different for each device. The curve of this profile is defined by a Bezier curve with four control points. These control points represent the start and end points of profiles A and D, in addition to points F and E (Fig. 4).

Here, the coordinates needed to define the kinematics of the mechanism are:

$$q = \{x_A,\ y_A,\ x_B,\ y_B,\ x_C,\ y_C,\ x_D,\ y_D,\ x_E,\ y_E,\ x_F,\ y_F,\ x_G,\ y_G,\ t,\ s\}. \tag{27}$$

Because the mechanism has one degree of freedom, 15 constraint equations are needed:

$$(x_A - x_B)^2 + (y_A - y_B)^2 - L_{AB}^2 = 0, \tag{28}$$

$$(x_A - x_C)^2 + (y_A - y_C)^2 - L_{AC}^2 = 0, \tag{29}$$

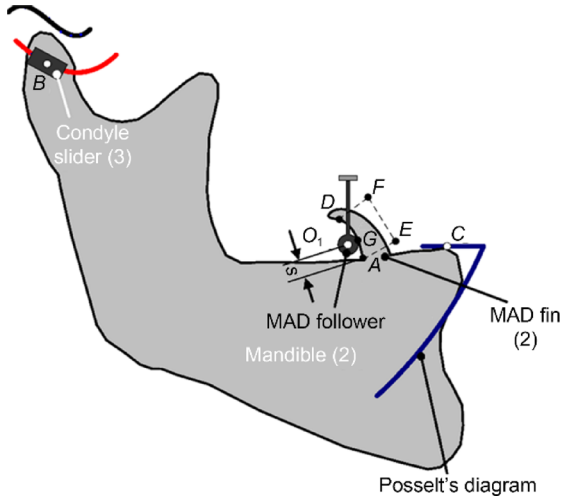

Fig. 4 Equivalent mechanism for a device with fins (Orthoapnea NOA). MAD: mandibular advancement device

$$(x_B - x_C)^2 + (y_B - y_C)^2 - L_{BC}^2 = 0, \tag{30}$$

$$(x_D - x_A) - \lambda_1(x_B - x_A) - \mu_1(x_C - x_A) = 0, \tag{31}$$

$$(y_D - y_A) - \lambda_1(y_B - y_A) - \mu_1(y_C - y_A) = 0, \tag{32}$$

$$(x_E - x_A) - \lambda_2(x_B - x_A) - \mu_2(x_C - x_A) = 0, \tag{33}$$

$$(y_E - y_A) - \lambda_2(y_B - y_A) - \mu_2(y_C - y_A) = 0, \tag{34}$$

$$(x_F - x_A) - \lambda_3(x_B - x_A) - \mu_3(x_C - x_A) = 0, \tag{35}$$

$$(y_F - y_A) - \lambda_3(y_B - y_A) - \mu_3(y_C - y_A) = 0, \tag{36}$$

$$\left(x_G - x_{O_1}\right)^2 + \left(y_G - y_{O_1}\right)^2 - L_{O_1G}^2 = 0, \tag{37}$$

$$y_B - \left(ax_B^3 + bx_B^2 + cx_B + d\right) = 0, \tag{38}$$

$$x_G - \left(a_x t^3 + b_x t^2 + c_x t + x_A\right) = 0, \tag{39}$$

$$y_G - \left(a_y t^3 + b_y t^2 + c_y t + y_A\right) = 0, \tag{40}$$

$$\left(x_G - x_{O_1}\right)\vartheta_x + \left(y_G - y_{O_1}\right)\vartheta_y = 0, \tag{41}$$

$$\left(x_A - x_{O_1}\right) - \frac{s}{L_{AD}}(x_D - x_A) = 0. \tag{42}$$

Equations (28)–(30) define the rigid solid condition of the lower jaw, as for previous cases. Equations (31) and (32) define the positions of the cam and point D in plane ABC. Similarly, Eqs. (33)–(36) define the positions of the control points of the cam curve, F and E, in the same plane. Moreover, parameters λ_i and μ_i are known ($i = 1, 2, 3$). Equation (37) indicates the rigid solid condition of the follower. Equation (38) specifies that point B must always remain on a curve along which the center of the condyle moves, as defined by the known parameters a, b, c, and d. Equations (39) and (40) state that the position of point G must be located on the Bezier curve of the cam profile, which is defined by points A, D, F, and E. Here, parameters a_x, b_x, c_x, a_y, b_y, and c_y are known and depend on the coordinates of points A, D, F, and E. Equation (41) states that vector O_1G and a tangent vector to the Bezier curve (ϑ) at point of contact G have perpendicular directions. Finally, Eq. (42) establishes the cam contact length.

Results

Once we established kinematic models for the most common mandibular advancement devices, we then analyzed their behavior in a patient according to the previously developed methodology. For all mandibular advancement devices shown in Fig. 5, we determined the curve followed by the tip of the lower incisor experimentally, and then compared this to the curve calculated using the kinematic model. A comparison of these two curves was then performed to validate the mathematical model presented in this work.

The trajectory followed by the tip of a patient's lower incisor during mouth opening was recorded while using each device (Fig. 5). The recording system used here included two Baumer VCXU-124C cameras and UV-A lamps (Fig. 6a). Two trihedrons with three markers each were attached to the upper and lower dental arches of each mandibular advancement device. The trihedrons were used to obtain the incisor trajectory, and were painted with a UV-fluorescent paint to simplify visualization under ultraviolet (UV) light (Fig. 6b). The trajectory was obtained using a self-developed image analysis program, so that the coordinates of the upper and lower trihedral markers were detected in each frame. With these coordinate data, we first obtained data characterizing the movement of the center of coordinates for each trihedron (i.e., points O_S and O_I). Next, using the method developed in Ref. [26], we determined the relative movement of the incisor with respect to the maxilla.

Devices with rigid bars

Figure 7 shows the movement sequence of the Panthera D-SAD device in which the trajectory of the lower incisor is visualized for the individual studied. This sequence was obtained for all devices analyzed here.

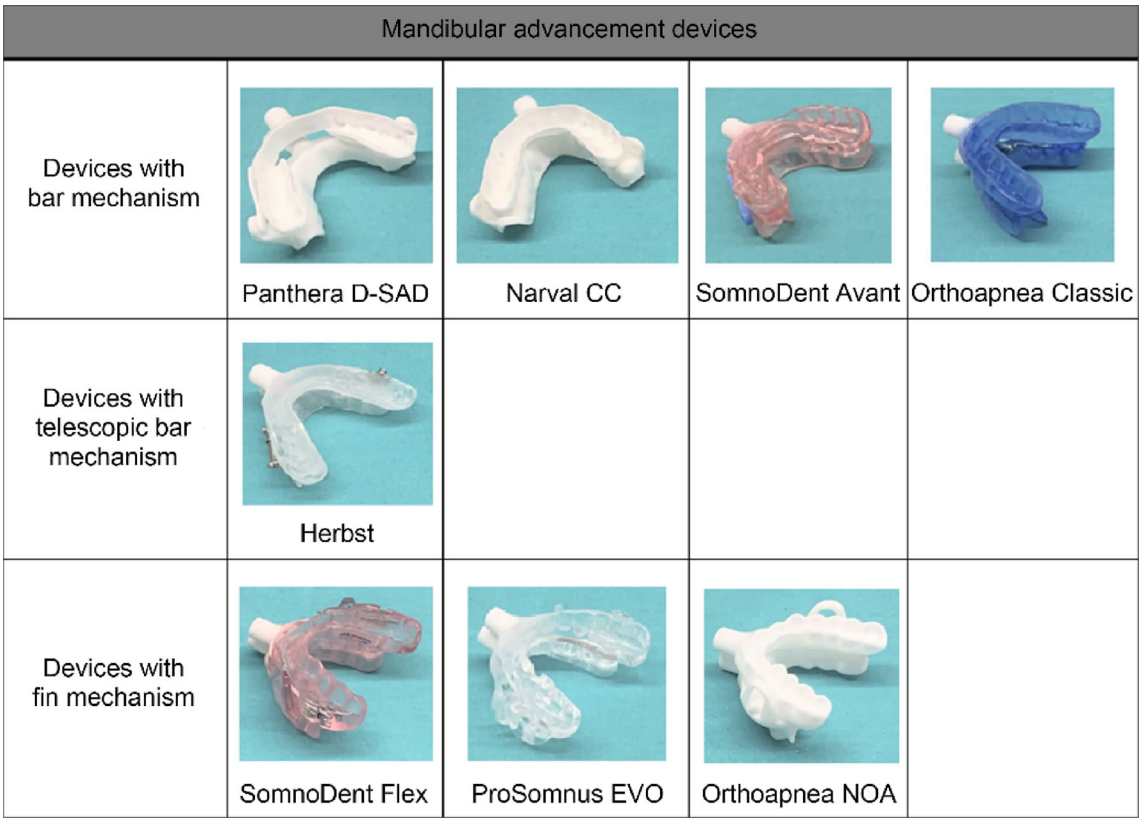

Fig. 5 Mandibular advancement devices examined in this study

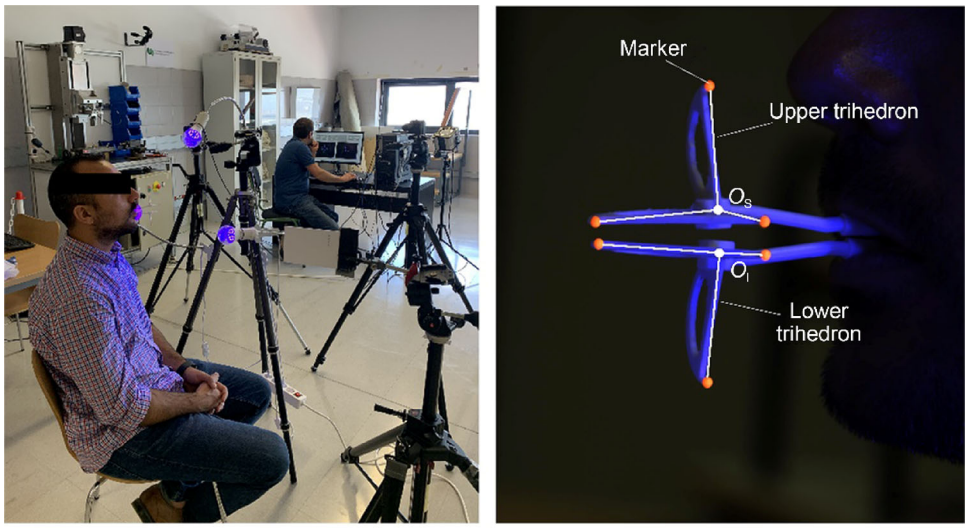

Fig. 6 Experimental MAD movement test: **a** real test; **b** frame obtained during patient test performance. MAD: mandibular advancement device

The results obtained for mandibular advancement devices with bars are shown in Figs. 8 and 9. In each figure, Posselt's patient diagram is represented in blue. This diagram shows the limits of the relative movement of the lower incisor with respect to the maxilla. The two borders that are most relevant to this study are: 1–2, since this specifies where the mandible moves forward while the mouth is closed without rotating, from the most retracted position (point 1) to the most advanced position (point 2); and 2–3 which shows where the mandible rotates when the condyle is located in the most advanced position.

As shown in Fig. 8, the trajectory of the lower incisor obtained mathematically for the MAD Panthera D-SAD model (shown in red) was compared with experimental data

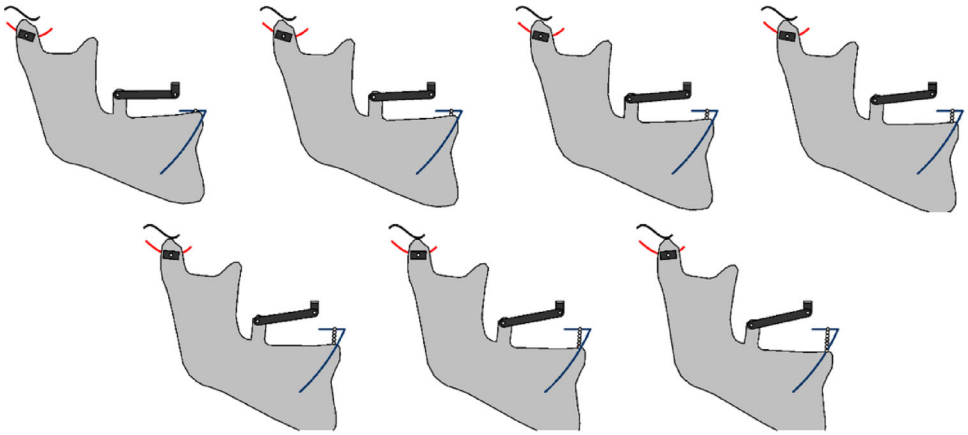

Fig. 7 Movement sequence of the Panthera D-SAD device

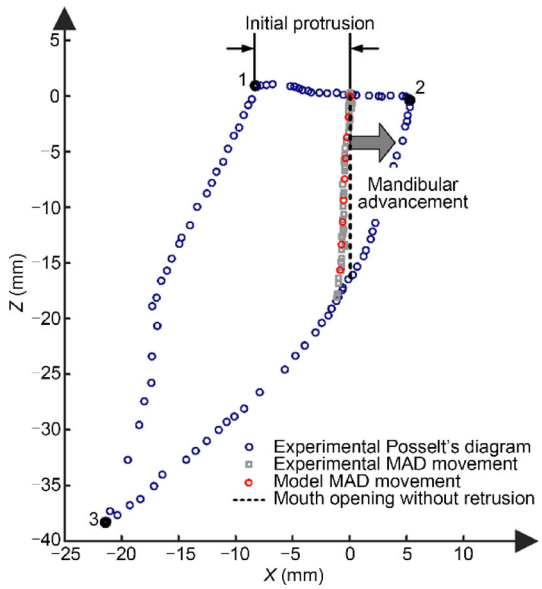

Fig. 8 Panthera D-SAD results. MAD: mandibular advancement device

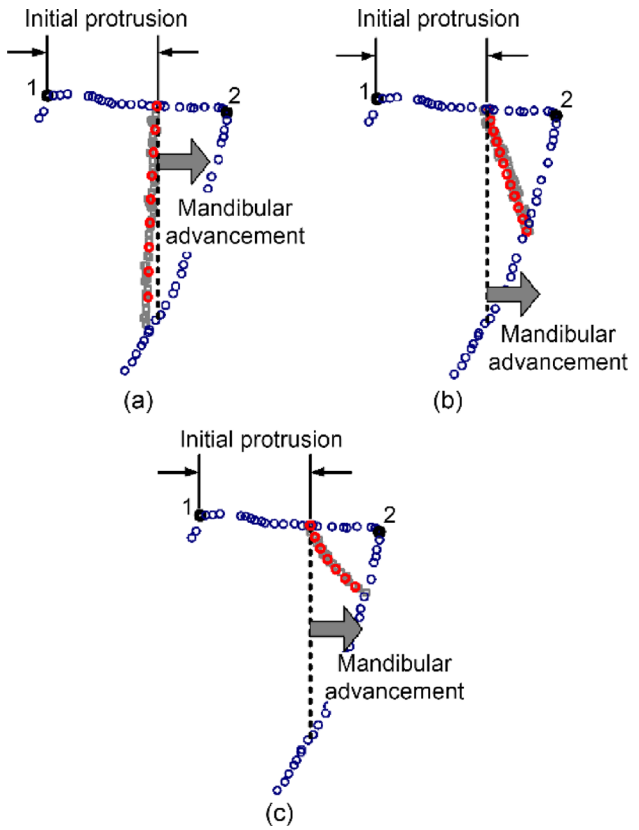

Fig. 9 Results for the following MADs with bars: **a** Narval CC; **b** SomnoDent Avant; **c** Orthoapnea Classic. MAD: mandibular advancement device

obtained using the camera system (shown in gray). This comparison showed a high degree of similarity indicating good model performance. For the first bar device, the trajectory followed by the incisor when opening the mouth deviated slightly from a vertical line passing through the starting point (i.e., 60% of the distance 1–2 for all devices). This vertical line represents the limit of movement from which the mandible begins to retract. Therefore, for the MAD Panthera D-SAD device, when the patient opens his/her mouth, the mandible retracts slightly with respect to its initial position.

For the other MADs with bars, we performed the same tests and the results are shown in Fig. 9. Figure 9a shows the results for the Narval CC device. As for the MAD Panthera D-SAD device, our mathematical model of Narval CC movement matched the experimental data closely, and a slight retrusion during opening the mouth was observed. Figures 9b and 9c show the results for the SomnoDent Avant and Orthoapnea Classic devices, respectively. In both cases, the mathematical model matched experimental data properly. Taken together, these results show that these two devices work properly during patient mouth opening, and that the mandible protrudes until the incisor reaches the anterior border of Posselt's diagram. It should be noted that since each of the four bar mechanisms analyzed has different positions for the joints of the kinematic pairs (i.e., O_2 and A) and different bar lengths (O_2A) (Table 1 and Fig. 10), the maximum degree

Table 1 Dimensions of the mechanism formed by the mandible and mandibular advancement devices (MADs) with bars

MAD	X_{O_2} (mm)	Y_{O_2} (mm)	L_{O_2A} (mm)	L_{BC} (mm)	L_{CA} (mm)	L_{AB} (mm)
Panthera D-SAD	0	0	30.62	97.62	41.92	57.41
Narval CC	0	0	27.80	97.62	39.64	60.00
SomnoDent Avant	0	0	53.11	97.62	31.44	74.12
Orthoapnea Classic	0	0	8.61	97.62	5.93	91.92

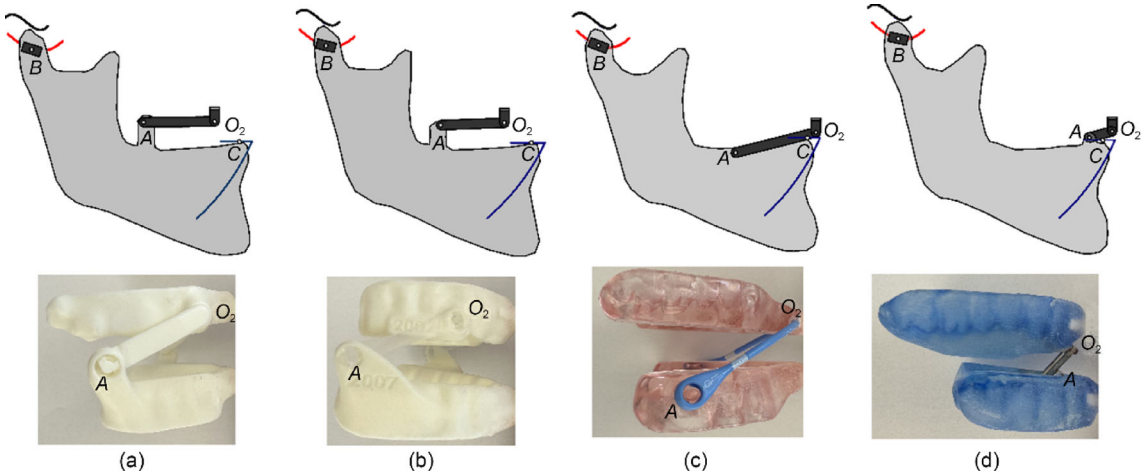

Fig. 10 MADs with bars: **a** Panthera D-SAD; **b** Narval CC; **c** SomnoDent Avant; **d** Orthoapnea Classic. MAD: mandibular advancement device

of mouth opening differs greatly. For example, the opening allowed by the Orthoapnea Classic device was the smallest (Fig. 9c), whereas that of the Panthera D-SAD device was the largest (Fig. 8).

Devices with telescopic bars

Next, mathematically determined trajectories of the lower incisor when the patient uses the Herbst device are shown in Fig. 11. The experimental results are not shown because the mechanism has two degrees of freedom, the lower incisor did not always follow the same trajectory, and therefore, the measurements differed among tests. For this test, when the patient opened his/her mouth while using this MAD, the telescopic bar can rotate a given angle γ and at the same time change its length (L_{O_2A}). Therefore, the movement of the lower incisor is not limited to one trajectory but to an area enclosed between two boundary trajectories. A more backward trajectory can be achieved by opening the mouth while maintaining the bar at its minimum length, i.e., by maintaining the initial value of variable s (Fig. 2). The most forward trajectory is described by lengthening the bar (i.e., L_{O_2A}) as much as possible for each angular position. Figure 11 shows in red the trajectory of the lower incisor obtained mathematically during mouth opening, keeping the initial value of variable s constant. Paths

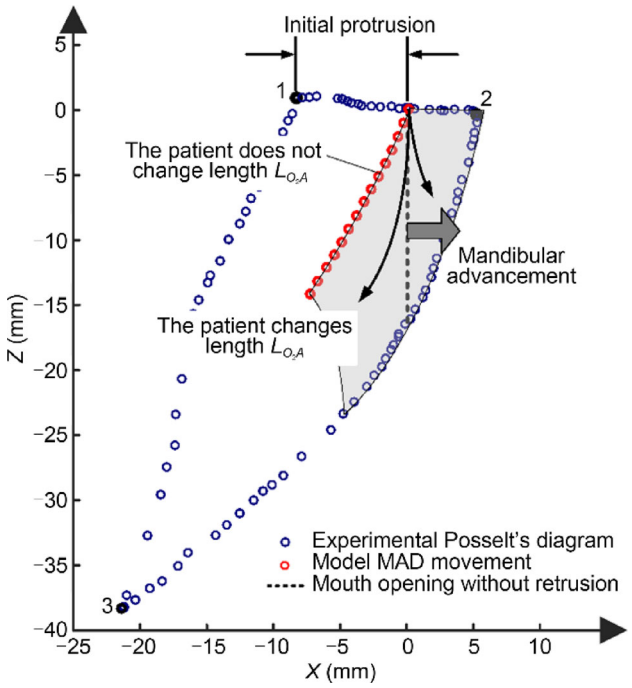

Fig. 11 Results for MADs with telescopic bars. MAD: mandibular advancement device

indicated by black arrows represent two possible trajectories for the incisor during mouth opening by increasing the values of variable s in two different ways that correspond to the two degrees of freedom. Accordingly, the incisor can move within the gray area shown in Fig. 11. This area is limited by a posterior border corresponding to the trajectory of the lower incisor while maintaining the minimum L_{O_2A} distance, and by a lower border characterized by the position of the incisor when the patient moves the lower jaw forward up to the maximum degree of mouth opening allowed by the device. The anterior and superior borders coincide with those of Posselt's.

Therefore, the operation of this device does not prevent retrusion of the mandible when the patient opens his/her mouth. This could lead to airway collapse, especially during sleep. To avoid retrusion, the patient should consciously control his/her position by increasing the value of variable s.

Devices with straight fins

Finally, we also obtained results for the most commonly used MADs with fins. Figure 12 shows results obtained for the SomnoDent Flex and ProSomnus EVO devices. The mathematically generated trajectory is shown in red, and the experimentally measured trajectory is shown in gray. Again, both trajectories show a strong match, indicating a high degree of model accuracy.

In both devices, the mandible recedes when the patient opens his/her mouth. Mandibular retraction was more pronounced in the SomnoDent Flex device (Fig. 12a) than in the ProSomnus EVO device (Fig. 12b). In addition, both devices have an opening limit position beyond which the lower fin is no longer in contact with the upper fin. This allows the patient to move his/her mandible freely. To avoid this problem, these devices are usually supplied with elastic straps that make it difficult to open the mouth.

Devices with curved fins (cams)

Figure 13 shows results for two Orthoapnea NOA devices designed from two different advancement curves. These devices, as mentioned above, are designed considering the specific morphologies of individual patients and the protrusive advancement curve predefined by the specialist. In other words, starting from the desired trajectory for the lower incisor, the cam is synthesized considering the mechanical system formed by the mandible and the device such that the lower incisor follows a specified trajectory.

Figure 13 shows, as for all previous cases, that the curve generated by our mathematical model (shown in red) closely matches experimentally measured data (shown in gray). This figure shows both an Orthoapnea NOA device designed using a curve with less protrusion when the mouth is opened, thereby allowing a large mouth opening (Fig. 13a), and another device with a larger protrusion and a correspondingly smaller mouth opening (Fig. 13b).

Discussion

To avoid variability in the trajectory of the condyle center during protrusion, retrusion, opening, and closing movements of the mandible, some authors proposed using the kinematic center as a reference point to reproduce the movement of the condyle [27]. However, the position of this point varies among individuals, and its precise location is not easy to obtain [28]. To simplify data collection and model development, the kinematic models presented in this paper calculate mandibular motion using the trajectory of the geometric center of the condyle and the rotation of the mandible around that point. From a kinematic point of view, this is rather simple, since planar movements of any object can be decomposed into the motion of a specific point plus the rotation of a body around that point. However, the computational identification of the trajectory of the geometric center of the condyle remains controversial. In this study, this center was considered to move with a trajectory whose distance to the glenoid fossa remained constant.

To test the impact of condyle motion variability on the kinematic model developed here, the trajectories of the lower incisor were calculated using different paths of the center of the condyle. We considered extreme cases, including where the condyle came into contact with the fossa or when the initial distance between the condyle and the fossa increased by more than 100%. Using these premises, we calculated the trajectories of the lower incisor for a variety of devices. The dispersion due to variation in the path of the center of the condyle was found not to be significant, and the kinematic model proposed here allowed us to determine the performance of each MAD in different individuals with an acceptable degree of accuracy. That is, we were able to determine whether the trajectory of the patient's incisor during mouth opening when using a given MAD was protrusive or retrusive, as well as to what degree. This was verified in the previous section, where we showed that the movement calculated for the lower incisor (point C) coincided with the movement measured experimentally in all cases (Figs. 8, 9, 11, 12, and 13).

After validation of the mathematical models, the trajectory of the incisor of any patient can be calculated using any device. This makes it possible to determine the kinematic behavior of a device depending on the patient's morphology before the start of treatment; such information can provide fundamental knowledge that can be used to improve the design of MADs.

All bar-based devices, such as those shown in Figs. 8 and 9, have similar mechanisms in which length L_{BC} depends on

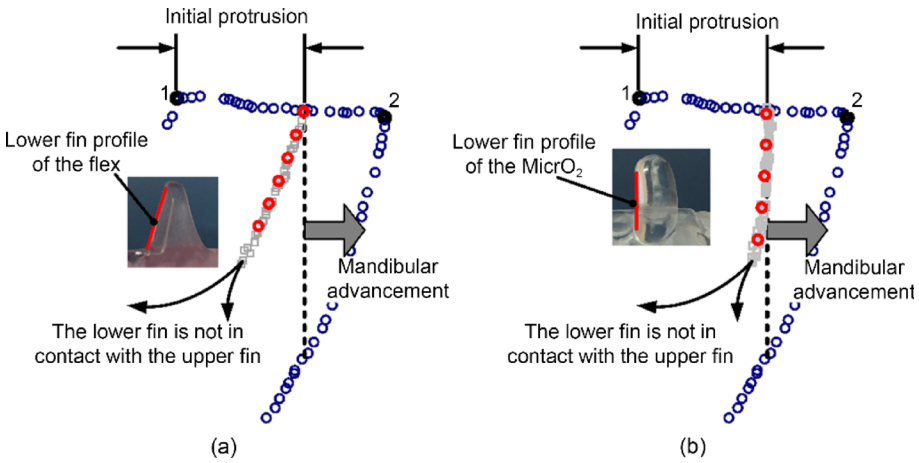

Fig. 12 **a** SomnoDent Flex; **b** ProSomnus EVO MicrO_2

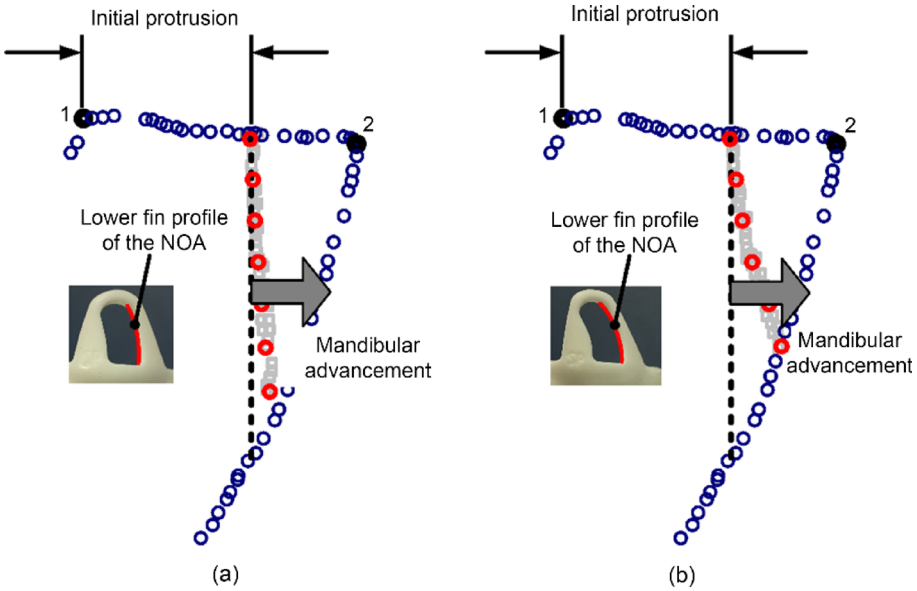

Fig. 13 Orthoapnea NOA MAD results: **a** less protruding curve; **b** more protruding curve. MAD: mandibular advancement device

the patient's morphology. Because in this work the behavior of all devices was studied using the same patient, the length L_{BC} did not vary among the analyzed mechanisms. For the same reason, the trajectory of the center of the condyle (point B) is the same for all cases because the curve of the glenoid fossa also did not vary. On the other hand, lengths L_{AB}, L_{CA}, and L_{O_2A} were different among different device trials, since these measurements depend on the design of each specific device (Table 1, Fig. 10). This is the reason why the different devices show different kinematic behaviors, even if they share equivalent mechanisms. In the case of the Panthera D-SAD and Narval CC models, when the patient opens his/her mouth, the mandible recedes (Figs. 8 and 9a), whereas for the SomnoDent Avant and Orthoapnea Classic models, opening causes the patient's mandible to protrude (Figs. 9b and 9c).

In general, if it is desirable that initial protrusion is maintained or even increased during opening of the mouth to avoid collapse of the upper airway when using a bar device, it is necessary to determine the length of the L_{O_2A} bar and the positions of points O_2 and A for each patient. This is because the same device used for different patients causes the trajectory of the tip of the incisor to be different. In addition to the fact that the shape and position of the glenoid fossa differ among patients, the assembly formed by the mandible and the device has different L_{BC}, L_{AB}, and L_{CA} distance values. Differences in trajectories are shown in Fig. 14, which compares incisor movement curves during mouth opening for two different patients when using the Narval CC device.

The Herbst telescopic rod device has two degrees of freedom, and therefore allows for multiple trajectories of the lower incisor during mouth opening. Thus, even if the device was designed considering the specific morphology of an individual patient, it is not possible to ensure that the incisor would have the same forward trajectory under all circumstances. Furthermore, when the patient is asleep, he/she is unable to control either the length of the bar (variable s) or

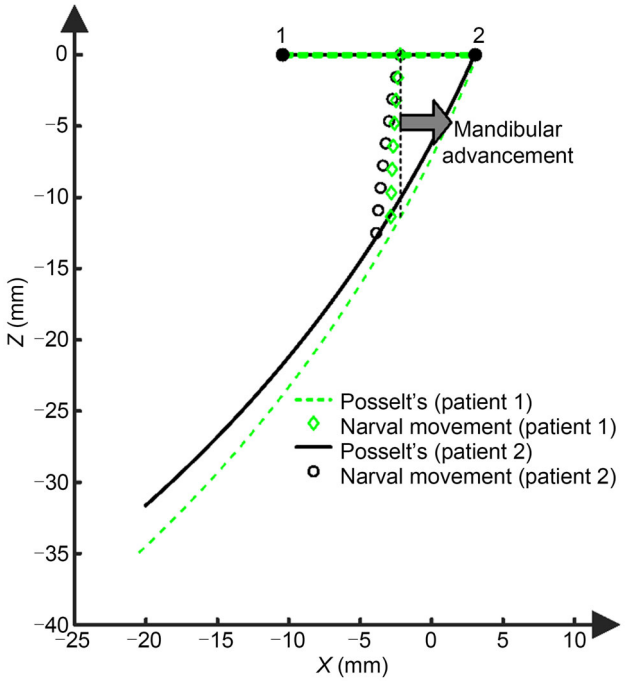

Fig. 14 Incisor trajectories of two different patients using the Narval CC MAD. MAD: mandibular advancement device

the mouth opening angle (variable γ). Therefore, regardless of the design of the device, in this device there will always be a retrusion of the mandible when opening the mouth, as shown in Fig. 11.

For devices with straight fins (Figs. 12 and 13), we first studied the SomnoDent Flex and ProSomnus EVO devices, which are among the most commonly used to treat sleep apnea. Moreover, due to the design of the fin profile (Fig. 12), they permit retrusion of the mandible when patients open their mouths. In addition, when the mouth opening reaches the limit of the fin, the mandible will move back to the resting position, since this is the most comfortable natural position for the patient. It should also be noted that these two devices do not consider individual patient morphologies. Therefore, the degree of lower jaw retraction when the mouth is opened can be more or less pronounced depending on the patient-specific morphological differences.

In the case of the Orthoapnea NOA device with curved cams, the design process ensures that the lower jaw does not retract when the mouth is opened. The design of the cam profile is done using a reverse process. That is, first, the specialist determines the desired advancement curve for the incisor within the borders of Posselt's envelope; next, using the patient's morphology data and the position of the follower in the upper splint, the exact profile of the cam can then be determined. In this way, control of lower jaw advancement can be achieved when patients open their mouths [11]. As shown in Fig. 13, the behavior of this device has been modeled using two different cam profiles, i.e., one that causes the mandible to barely advance during mouth opening (Fig. 13a) and the other that permits a more pronounced advancement (Fig. 13b).

Given these results, we can answer the question raised at the beginning of this paper, namely, if the purpose of these devices is to avoid upper airway collapse by keeping the mandible in a forward position, why do some devices move the mandible backward when patients open their mouths? We first note that specialists determine the degree of initial protrusion that is convenient for each patient when his/her mouth is closed (Fig. 8). Therefore, we can state that all devices are equally effective with the mouth closed, and that any problem appears when opening the mouth. For this reason, some devices mount vertical elastic bands between the upper and lower splints to minimize the degree of mouth opening. Moreover, many investigations have examined the influence of limiting mouth opening on treatment outcomes. In some cases, no appreciable difference has been found between limiting mouth opening and not mouth opening [29]. However, others have concluded that minimizing mouth opening enhances treatment outcomes [30]. The explanation for this disparity is simple. In the first case, the Narval CC device was used, which barely retracts the mandible during mouth opening (Fig. 9a). In contrast, in the second case, the MAD used was a Somnodent model, which produces a very significant retrusion (Fig. 12a). The only customization common to all MADs considers the initial protrusion and dental arches. From there, each device has a mechanical solution to control lower jaw movement that is applicable to all patients. However, a complete design must consider that the mandible is part of the mechanical system. Therefore, the mandible must be considered along with the coupling system between the splints. Most devices have one degree of freedom. Therefore, the mechanical assembly formed by the jaw and the device mechanism completely determines the trajectory of the incisor. However, because the mechanical assembly depends on an individual patient's morphology, a mechanism that advances the mandible in one individual during mouth opening may actually retract it in another. To solve this problem, the authors propose studying the complete mechanical assembly of the jaw together with the MAD and performing a dimensional synthesis process, in which the tip of the lower incisor is the follower that has to move on a trajectory predefined by the specialist. Moreover, for MADs with fins, this process has been performed in another study by the authors of this work [11], and has permitted the design of the Orthoapnea NOA device.

Conclusions

In this study, the kinematics of the mandible when using a mandibular advancement device was studied. The kinematic model of the mechanisms used by different common MADs was then validated using experimental tests. Our results established the importance of considering patient morphology for optimal MAD design, and addressed how some devices work improperly when patients open their mouths. As demonstrated here, although all MADs studied work correctly when the patient's mouth is closed, some perform inadequately when the mouth is open. An obvious solution is to use monoblock MADs that prevent the mouth from opening; however, these devices are uncomfortable and have a high rate of rejection by patients relative to devices that allow mouth opening.

Given the importance of two-piece mandibular advancement devices for treating sleep apnea, it is important that they are designed correctly. In general, it is necessary to consider the specific morphological differences of patient mandibles and to use this information to more effectively model the kinematic pairs of the MAD.

Acknowledgements A substantial part of this work was supported by the research contracts 806/31.4830 and 806/31.5511 between the private company Laboratorio Ortoplus S.L. and the University of Malaga.

Author contributions Conceptualization and methodology: MG, JAC, and AB; investigation: all authors; writing—original draft: JAC and AB; writing—review and editing: all authors.

Funding Funding for open access publishing: Universidad Málaga/CBUA.

Declarations

Conflict of interest On behalf of all authors, the corresponding author states that there is no conflict of interest.

Ethical approval This article does not contain any studies with human or animal subjects performed by any of the authors.

References

1. Dempsey JA, Veasey SC, Morgan BJ et al (2010) Pathophysiology of sleep apnea. Physiol Rev 90(1):47–112. https://doi.org/10.1152/physrev.00043.2008
2. Malhotra A, White DP (2002) Obstructive sleep apnoea. Lancet 360(9328):237–245. https://doi.org/10.1016/S0140-6736(02)09464-3
3. Bradley TD, Floras JS (2009) Obstructive sleep apnoea and its cardiovascular consequences. Lancet 373(9657):82–93. https://doi.org/10.1016/S0140-6736(08)61622-0
4. Wang HQ, Newton JD, Floras JS et al (2007) Influence of obstructive sleep apnea on mortality in patients with heart failure. J Am Coll Cardiol 49(15):1625–1631. https://doi.org/10.1016/j.jacc.2006.12.046
5. Yaggi HK, Concato J, Kernan WN et al (2005) Obstructive sleep apnea as a risk factor for stroke and death. New Engl J Med 353(19):2034–2041. https://doi.org/10.1056/NEJMoa043104
6. Glos M, Penzel T, Schoebel C et al (2016) Comparison of effects of OSA treatment by MAD and by CPAP on cardiac autonomic function during daytime. Sleep Breath 20(2):635–646. https://doi.org/10.1007/s11325-015-1265-0
7. Venema JAMU, Rosenmöller BRAM, de Vries N et al (2021) Mandibular advancement device design: a systematic review on outcomes in obstructive sleep apnea treatment. Sleep Med Rev 60:101557. https://doi.org/10.1016/j.smrv.2021.101557
8. Dieltjens M, Vanderveken OM, van de Heyning PH et al (2012) Current opinions and clinical practice in the titration of oral appliances in the treatment of sleep-disordered breathing. Sleep Med Rev 16(2):177–185. https://doi.org/10.1016/j.smrv.2011.06.002
9. Sanz PM, Reyes MG, Torras AB et al (2021) Craniofacial morphology/phenotypes influence on mandibular range of movement in the design of a mandibular advancement device. BMC Oral Health 21(1):2–10. https://doi.org/10.1186/s12903-020-01369-z
10. Bloch KE, Iseli A, Zhang JN et al (2000) A randomized, controlled crossover trial of two oral appliances for sleep apnea treatment. Am J Respir Crit Care Med 162(1):246–251. https://doi.org/10.1164/ajrccm.162.1.9908112
11. Yow M (2009) An overview of oral appliances and managing the airway in obstructive sleep apnea. Semin Orthod 15(2):88–93. https://doi.org/10.1053/j.sodo.2009.01.006
12. Bataller A, Cabrera JA, García M et al (2018) Cam synthesis applied to the design of a customized mandibular advancement device for the treatment of obstructive sleep apnea. Mech Mach Theory 123:153–165. https://doi.org/10.1016/j.mechmachtheory.2018.02.002
13. Xu WL, Bronlund JE, Potgieter J et al (2008) Review of a human masticatory system and masticatory robotics. Mech Mach Theory 43(11):1353–1375. https://doi.org/10.1016/j.mechmachtheory.2008.06.003
14. Daumas B, Xu WL, Bronlund J (2005) Jaw mechanism modeling and simulation. Mech Mach Theory 40(7):821–833. https://doi.org/10.1016/j.mechmachtheory.2004.12.011
15. Delsignore MJ, Krovi VN (2008) Screw-theoretic analysis models for felid jaw mechanisms. Mech Mach Theory 43(2):147–159. https://doi.org/10.1016/j.mechmachtheory.2007.02.005
16. Xu WL, Lewis D, Bronlund JE et al (2008) Mechanism, design and motion control of a linkage chewing device for food evaluation. Mech Mach Theory 43(3):376–389. https://doi.org/10.1016/j.mechmachtheory.2007.03.004
17. Cheng C, Liu B, Li YN et al (2022) Elastodynamic performance of a spatial redundantly actuated parallel mechanism constrained by two point-contact higher kinematic pairs via a model reduction technique. Mech Mach Theory 167:1–25. https://doi.org/10.1016/j.mechmachtheory.2021.104570

18. Xu WL, Bronlund JE (2010) Mastication Robots: Biological Inspiration to Implementation. Springer, Berlin. https://doi.org/10.1007/978-3-540-93903-0
19. Posselt U (1952) Studies in the mobility of the human mandible. Acta Odontol Scand 10(Suppl):19–160
20. Yuan FS, Sui HX, Li ZK et al (2015) A method of three-dimensional recording of mandibular movement based on two-dimensional image feature extraction. PLoS ONE 10(9):e0137507. https://doi.org/10.1371/journal.pone.0137507
21. Fang JJ, Kuo TH (2008) Modelling of mandibular movement. Comput Biol Med 38(11):1152–1162. https://doi.org/10.1016/j.compbiomed.2008.09.001
22. Enciso R, Memon A, Fidaleo DA et al (2003) The virtual craniofacial patient: 3D jaw modeling and animation. Stud Health Technol Inform 94:65–71. https://doi.org/10.3233/978-1-60750-938-7-65
23. Pinheiro AP, Pereira AA, Andrade AO et al (2011) Measurement of jaw motion: the proposal of a simple and accurate method. J Med Eng Technol 35(3–4):125–133. https://doi.org/10.3109/03091902.2010.542270
24. García Reyes M, Bataller Torras A, Cabrera Carrillo JA et al (2022) A study of tensile and bending properties of 3D-printed biocompatible materials used in dental appliances. J Mater Sci 57(4):2953–2968. https://doi.org/10.1007/s10853-021-06811-3
25. García de Jalón J, Bayo E (2011) Kinematic and Dynamic Simulation of Multibody System. Springer, New York. https://doi.org/10.1007/978-1-4612-2600-0
26. García M, Cabrera JA, Bataller A et al (2021) 3D kinematic mandible model to design mandibular advancement devices for the treatment of obstructive sleep apnea. Bio-Des Manuf 4(1):22–32. https://doi.org/10.1007/s42242-020-00101-8
27. Yatabe M, Zwijnenburg AJ, Megens CCE et al (1995) The kinematic center: a reference for condylar movements. J Dent Res 74(10):1644–1648. https://doi.org/10.1177/00220345950740100401
28. Gallo LM, Gössi DB, Colombo V et al (2008) Relationship between kinematic center and TMJ anatomy and function. J Dent Res 87(8):726–730. https://doi.org/10.1177/154405910808700810
29. Norrhem N, Marklund M (2013) An oral appliance with or without elastic bands to control mouth opening during sleep—a randomized pilot study. Sleep Breath 20(3):929–938. https://doi.org/10.1007/s11325-016-1312-5
30. Milano F, Mutinelli S, Sutherland K et al (2018) Influence of vertical mouth opening on oral appliance treatment outcome in positional obstructive sleep apnea. J Dent Sleep Med 5(1):17–23. https://doi.org/10.15331/jdsm.6918